

The stress assisted evolution of point and extended defects in silicon

Samir Chaudhry^{a)} and Mark E. Law

Department of Electrical and Computer Engineering, University of Florida, Gainesville, Florida 32611

(Received 21 January 1997; accepted for publication 5 May 1997)

As semiconductor devices are scaled to sub-micron dimensions, they are becoming more complex in geometry and materials. Stress related problems are therefore pervasive and critical in ultralarge scale integrated technology. High levels of stress can cause severe degradation of device characteristics by generating and propagating dislocations in the silicon substrate. Furthermore, stress in the silicon substrate can cause dopant redistribution to an extent it can no longer be neglected when designing scaled devices. In this study the effect of stress, generated from patterned nitride stripes on silicon, on the diffusion of phosphorus and evolution of ion-implanted dislocation loops is investigated. Phosphorus displays retarded diffusion, while the dislocation loops are smaller and less dense in the compressive regions under the nitride film. © 1997 American Institute of Physics. [S0021-8979(97)06715-7]

INTRODUCTION

Continued shrinkage of silicon device dimensions and increasing complexity of device processing has led to an increase in stress levels in the active regions of silicon devices. The stress can alter diffusion kinetics of implanted dopants and in some instances lead to the formation of extended defects. The primary goal of this study is to investigate the effects of stress on dopant diffusion and extended defect evolution. In addition, a quantitative model, which can be used to predict the effect of stress in more general situations, is developed and implemented into a process simulator.

Investigations of several researchers have revealed that phosphorus and boron exhibit retarded diffusion when annealed under a deposited nitride layer.¹⁻³ As early as 1982, Mizuo and Higuchi¹ observed anomalous diffusion of boron and phosphorus in silicon under chemical vapor deposited (CVD) nitride films. They discovered that in an inert atmosphere the diffusion of these dopants under CVD nitride films is retarded compared to the diffusion under the SiO₂ films covered with CVD nitride. Their results indicated that the Si-SiO₂ interface could be acting as a sink for supersaturated interstitials. However, they neglected the high levels of stress in the nitride film, and theorized that the deposited nitride film was inert, with regards to perturbing point defect concentrations in the bulk. Ahn *et al.*² observed a vacancy supersaturation and a self-interstitial undersaturation under low pressure chemical vapor deposited (LPCVD) nitride with tensile stress. The degree of super or undersaturation of point defects was found to be closely related to the stress level in the silicon nitride film. They further theorized that the nitride film was generating vacancies by absorbing silicon atoms at the interface to relieve its own tensile stress. Osada *et al.*³ investigated the effect of an LPCVD nitride on boron diffusion in the substrate below. They observed that as long as the nitride thickness was greater than 50 Å, boron diffusion was retarded under the nitride film, when compared to a region where an oxide film was under an overlying ni-

tride. In addition, this retardation in boron diffusion was found to increase with increasing nitride film thickness and decreasing anneal temperature. The results were explained solely due to compressive stress in the substrate below the tensile deposited film, which lead to an undersaturation of vacancies. Kuo *et al.*⁴ investigated boron diffusion in Si and Si_{1-x}Ge_x. They observed slower boron diffusion in compressively strained Si_{1-x}Ge_x, when compared to unstrained silicon, and attributed it to an increase in interstitial formation energy in the compressive Si_{1-x}Ge_x. However, the intrinsic boron diffusivities in Si_{0.80}Ge_{0.20} and Si_{0.90}Ge_{0.10} exhibited weak strain dependence, suggesting that the boron diffusivity in Si_{1-x}Ge_x is predominantly a function of Ge content.

Since both phosphorus and boron diffuse mainly through an interstitial mechanism, it has been suggested that the compressive stress in the substrate immediately below the tensile nitride layer leads to an undersaturation of interstitials, which would explain the retarded diffusion. The research, described in the preceding paragraph, suggests that the stress in the nitride film has a significant effect on bulk diffusion properties. A comprehensive look at the diffusion properties of a representative dopant, as a function of film thickness and stripe width, would not only greatly enhance the understanding of stress-assisted diffusion, but also allow the calibration of process simulators like Florida object oriented process simulator (FLOOPS). FLOOPS allows simulation of semiconductor device processing in one, two, or three dimensions. It uses finite element analysis to determine the magnitude of stress from sources such as deposited films. These simulations are quite accurate as they use the standard finite element technique to solve the balance of forces equation. However, the effect of a given stress field on variables such as dopant diffusivities needs to be calibrated. In order to facilitate such calibration, an experiment is designed to introduce stress in the silicon substrate in a predetermined way. Finite element stress simulations in FLOOPS (Fig. 1) revealed that patterned nitride films introduce both compressive and tensile stress in the substrate. The stress levels in the substrate are a strong function of nitride film thickness and stripe width. Thus, such structures would be extremely use-

^{a)}Current address: Bell Laboratories (Lucent Technologies), 9333 S. John Young Pkwy, Orlando, FL 32819; Electronic mail: schaudhry@lucent.com

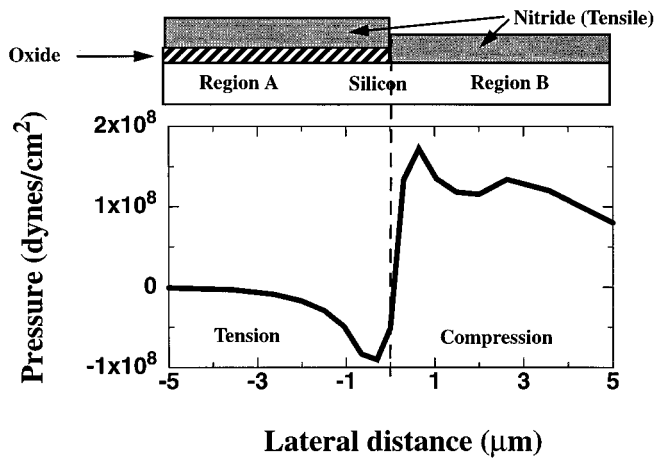


FIG. 1. Finite element simulation of the hydrostatic pressure under a nitride stripe in FLOOPS illustrating the regions of compression (under nitride) and tension (under the oxide padded nitride).

ful in observing the effect of both compression and tension simultaneously on bulk processing variables. In contrast to the work of Ahn *et al.*,² results from such a study could be analyzed directly using a finite element stress solver in process simulators like FLOOPS.

The discussion in the preceding paragraphs focused on stress-assisted diffusion of phosphorus and boron; the kinetics being dominated by point defect concentrations in the bulk. With extensive use of ion implantation in modern devices, type-II loops are frequently encountered in silicon technology. Since dislocation loop evolution is strongly governed by the point defects concentrations in the bulk, it seems reasonable to assume that stress in the substrate would have some effect on the evolution kinetics of ion-implanted dislocation loops. For example, a trench is known to introduce both compressive and tensile stress in substrate adjacent to it (Fig. 2). An experiment which simultaneously investigates the effect of compression and tension on the evolution of dislocation loops, would, therefore, be of great aid to process and device engineers designing new devices or improving old ones.

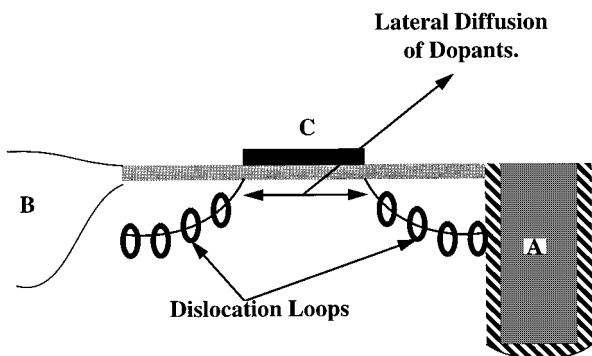


FIG. 2. A representative diagram of a metal oxide semiconductor field-effect transistor (MOSFET) with its possible isolation schemes, showing the location of dislocation loops and dopants. A, B, and C are the possible sources of stress that may influence the evolution of dislocation loops or the diffusion of dopants.

An experimental procedure is designed to investigate the effects of stress on the evolution of dislocation loops and on the diffusion of phosphorus as a representative dopant. A series of nitride stripes are used to generate alternating tensile and compressive stress fields in the substrate. The diffusion of phosphorus under the masked and unmasked regions is compared using the standard junction staining technique. The evolution of the dislocation loops with anneal time is monitored using the transmission electron microscopy (TEM) technique. Although both the phosphorus diffusion and dislocation loop experiments were performed in parallel, for the sake of clarity the results are discussed in separate sections.

II. EXPERIMENTAL DETAILS

p-type boron doped (15–25 Ω resistivity) Czochralski $\langle 100 \rangle$ oriented wafers were used for the study. The wafers were annealed in dry oxygen for 60 min to grow a 300 \AA oxide. Ellipsometric measurements were utilized to confirm that the thickness of the oxide did not appreciably change on the same wafer as well as from wafer to wafer. The oxide initially served as a screen from ion implantation and subsequently as a diffusion mask to prevent loss of dopant during annealing. A Varian ion beam implanter was used to implant phosphorus into half the silicon wafers through the screen oxide. High dose diffusions effects during the subsequent anneal were eliminated by utilizing a dose ($1 \times 10^{14}/\text{cm}^2$) below the amorphizing threshold of silicon. The energy of the implant (100 keV) was chosen to match standard implantation procedures in modern complementary metal oxide semiconductor (CMOS) processes. Under these implant conditions the dopant redistributed itself in a 1- μm -deep region in the silicon substrate. This would aid subsequent cleaving of the samples for junction measurements. The wafers were then subjected to a 30 min/900 $^\circ\text{C}$ anneal to remove the implantation damage and activate the implanted dopant. The second set of wafers received a silicon implant ($1 \times 10^{15}/\text{cm}^2$, 50 keV). The implant conditions were chosen so as to amorphize the substrate to a depth of ~ 1300 \AA . During subsequent anneals type-II dislocation loops would be formed at this depth.

A spin on technique (3500 rpm/25 s) was used to deposit an I-line photoresist on the oxide coated wafers. A photolithographic stepper then patterned stripes ranging in width from 1–1000 μm on the photoresist. Using the photoresist as a mask, a 10:1 buffered hydrofluoride etch was employed to create corresponding stripes in the oxide layer. The lateral etch was insignificant since the thickness of the oxide was 0.03 μm . The remaining photoresist was then removed by boiling the wafers in 110 $^\circ\text{C}$ solution of sulfuric acid and hydrogen peroxide.

A LPCVD silicon nitride was deposited on the wafers to generate the stress in the substrate. The nitridation was performed at 900 $^\circ\text{C}$ /211 mTorr. The following flow rates were used for the various gases during the process; nitrogen: 48 sccm; SiHCl_2 : 60 sccm; Ammonia: 882 sccm. The flow rates were chosen to match stress calibrated nitrides found in the literature.⁵ Under these conditions it is estimated that the

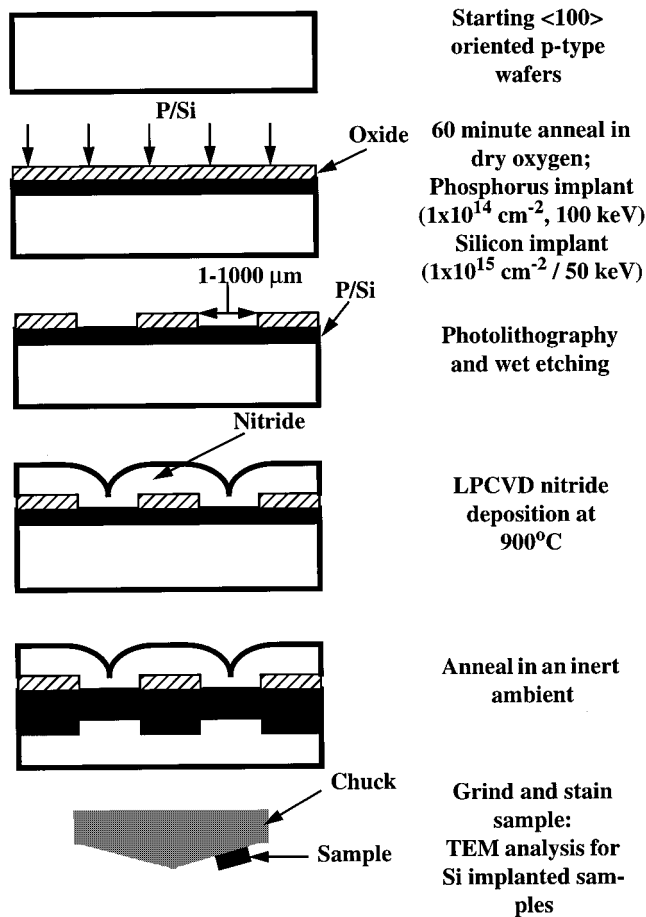


FIG. 3. Flow schematic of the experiment designed to study the effect of nitride stripes on the diffusion of phosphorus and evolution of ion-implanted dislocation loops in silicon.

stress levels in the nitride are of the order of $1 - 5 \times 10^9$ dynes/cm². Simulations in FLOOPS⁶ suggest that this would generate sufficient stress in the silicon substrate to observe the effects under investigation. The stress levels, however, would remain below the yield strength of silicon. The phosphorus samples were then annealed in a nitrogen ambient at 1000°C for times ranging from 2 to 4 h. The silicon implanted samples were annealed at a lower temperature (900°C) to prevent rapid dissolution of the dislocation loops.⁷ A flow chart depicting the entire experiment is shown in Fig. 3. The phosphorus samples were analyzed using the junction staining technique, while TEM was employed to investigate the evolution of dislocation loops. The two techniques are briefly described in the subsections below.

A. Junction staining

As discussed earlier compressive stress below the nitride stripes and tensile stress outside the stripes would alter the diffusion kinetics of the dopant. Since the dimensions of the stripes range from 1 to $1000 \mu\text{m}$ a convenient method to quantify the diffusion would be to use a junction staining technique to demarcate the junctions. The samples were initially cut into ~ 3 mm square pieces. They were mounted on a stainless steel chuck with a cleaving angle of ~ 17 min. The angle was chosen in view of the fact that the predomi-

nant diffusion is within a micron of the surface. A diamond compound on a glass plate was used as the grinding surface. Upon cleaving a chemical stain was used to demarcate the n -type dopant. The samples were placed under an optical microscope and two junction depths (one representing the diffusion under the nitride film, and the other representing diffusion under the oxide/nitride films) were measured for each sample using the micrometer scales on the microscope.

B. Transmission electron microscopy

The silicon implanted samples were mechanically lapped and jet etched for observation under a JEOL 200CX TEM. The analysis was performed using weak-beam dark field (g_{220}) image of the samples. By measuring loop size and their numbers in plan view, it was possible to determine quantitatively the total density of the loops, their radii, and the concentration of atoms trapped in the loops. Assuming a circular loop, the radius of each loop was measured along its longest axis and the corresponding loop area was calculated. The concentration of atoms bound by the loops is estimated by multiplying the fraction of the loop area by the atomic density in the $\langle 111 \rangle$ plane ($1.5 \times 10^{15}/\text{cm}^2$).

III. EXPERIMENTAL RESULTS

Experimental results from the phosphorus and silicon implanted samples are discussed in the Secs. III A and III B. Section III A brings out the effect of nitride stripes on point defects. Section III B elucidates the effect of identical nitride stripes on extended defects (ion-implanted dislocation loops).

A. Phosphorus implanted samples

Figure 4 illustrates the effect of the nitride stripes on the diffusion of phosphorus in silicon, which is quantitatively represented as ΔX_j . It is the difference between the junction depth under a nitride stripe (i.e., the region where the nitride is directly on top of the silicon) and outside it (i.e., the region where an oxide layer is padded between the nitride layer and the silicon substrate). The trends are quite apparent. As the thickness of the nitride layer is increased, the net retardation (ΔX_j) increases. An increase in the stripe width for the same nitride thickness also causes ΔX_j to increase.

B. Silicon implanted samples

Two fundamental figures of merit used to quantify a dislocation loop ensemble are its total density (D_{all}) and the average radius (R_{ave}). Earlier work quantified their evolution in an inert ambient.⁷ This study focuses on the net variation in these quantities from region A to region B (Fig. 1). Figure 5(a) shows a dark field plan view TEM microphotograph under the compressed region (region B) of a $20 \mu\text{m}$ stripe width sample. Figure 5(b) is a similar plan view under the tensed region (region A) of the same sample. The thickness of the nitride film is 1000 \AA , and the sample was annealed for 90 min at 900°C . The loops are consistently found to be sparser and smaller under a nitride layer, i.e.,

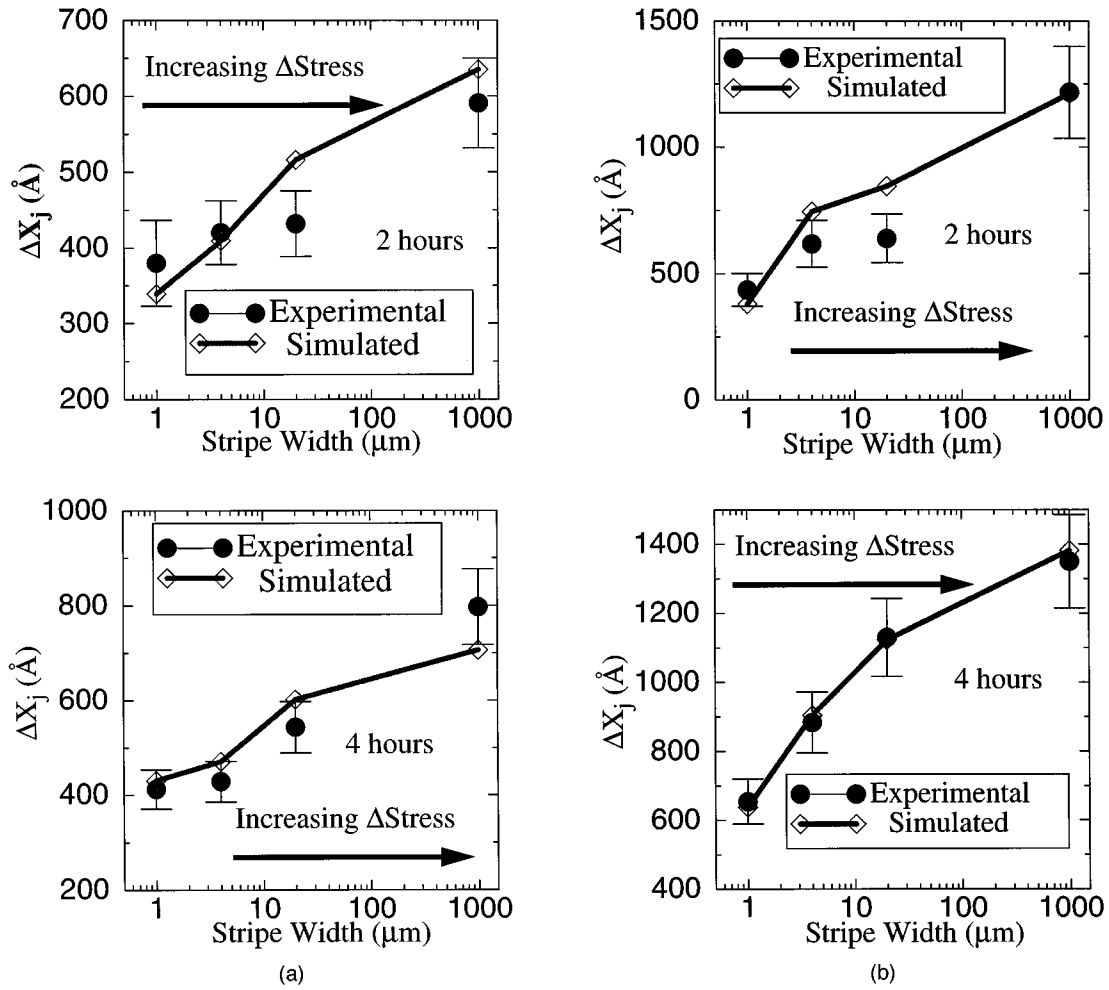


FIG. 4. Plot illustrating the effect of nitride stripe width and thickness on the net retardation of phosphorus diffusion: (a) 1000 Å nitride film and (b) 2000 Å nitride film.

$$D_{\text{all}}(A) > D_{\text{all}}(B), \quad (1)$$

$$R_{\text{ave}}(A) > R_{\text{ave}}(B), \quad (2)$$

where D_{all} is the total density of loops, and R_{ave} is the average radius of the loops.

IV. DATA ANALYSIS AND MODELING

The effects of patterned nitride films on the diffusion of phosphorus and the evolution of dislocation loops were experimentally investigated in the previous sections. The diffusion of phosphorus was retarded in regions of compression and enhanced in regions of tension. The dislocation loops were found to be sparser and smaller in regions of compression when compared to the adjacent tensile regions. The experimental results are analyzed and modeled in Secs. IV A and IV B.

A. Simulation of the stress-assisted diffusion of phosphorus

Tensile stress is known to exist in the LPCVD deposited nitride film.⁵ This stress leads to a compressive stress field immediately below the nitride film (finite element stress simulations in FLOOPS—Fig. 1). In the regions where an oxide film pads off the overlying nitride film the substrate is

under tension. The equilibrium concentration of point defects is changed by the presence of this stress field, and is quantitatively represented as

$$C_I^*(P) = C_I^*(P=0) \exp\left(\frac{-P\Delta V_I}{kT}\right), \quad (3)$$

$$C_V^*(P) = C_V^*(P=0) \exp\left(\frac{P\Delta V_V}{kT}\right), \quad (4)$$

where $C_{I/V}^*(P)$ is the equilibrium concentration of interstitials/vacancies in the presence of the pressure field, P is the spatially dependent magnitude of the pressure field, k is the Boltzmann's constant, and T is the temperature. ΔV_I and ΔV_V are effective interstitial and vacancy expansion volumes, and are defined as

$$\Delta V_I = 1.33\pi\epsilon r_o^3, \quad (5)$$

$$\Delta V_V = 2\pi r_s^2 \gamma \Gamma / \mu, \quad (6)$$

where r_o and ϵ are the radius and dilatation of the dopant atom, r_s and Γ are the radius and surface tension of the vacancy well, respectively, μ is the shear modulus of silicon, and γ is related to the Poisson's ratio η of the material ($=0.3$ for silicon) as

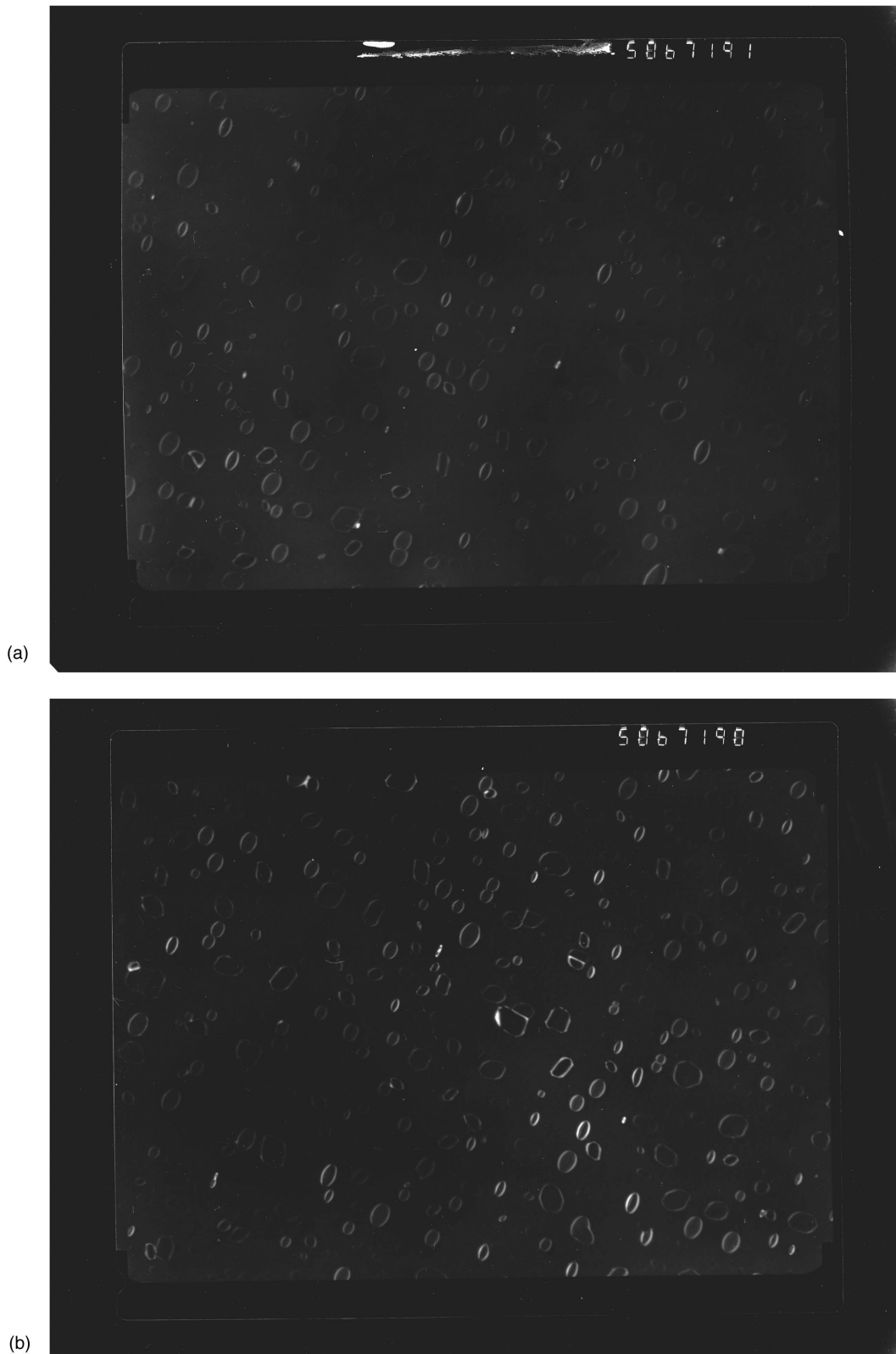


FIG. 5. Dark field plan view TEM microphotographs ($\times 50\,000$ magnification) for a sample with a nitride stripe width of $20\ \mu\text{m}$, and a thickness of $1000\ \text{\AA}$; under (a) compressive (region B) and (b) tensile (region A) regions. Note the significant difference in the size and density of the loops in the two regions.

$$\gamma = 3.0 \cdot \frac{1 - \eta}{1 + \eta} \quad (7)$$

Stress simulations in FLOOPS suggested that increase in the thickness of the deposited nitride layer would lead to

higher levels of stress in the substrate below the layers. This explains the added retardation observed in the experimental data as the thickness of the nitride layer was increased. These results do not qualitatively agree with the data of Ahn *et al.*²

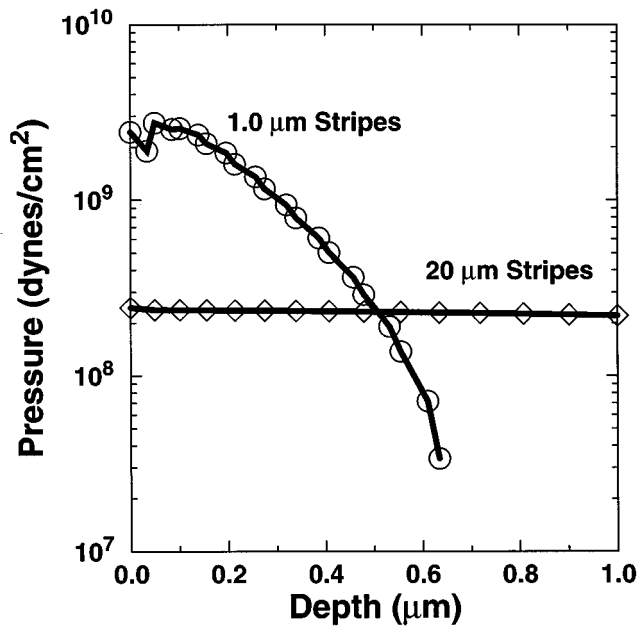


FIG. 6. Plots of pressure, as a function of depth in the silicon substrate, in the middle of the stripe, for various stripe widths, and a nitride film thickness of $0.1 \mu\text{m}$. As the stripes get smaller and closer, the compressive and tensile pressure peaks get bigger in magnitude, indicating the effect of the neighboring stripes. However, deeper in the substrate stress from the wider stripes is higher.

In their study the retardation was found to remain constant with an increase in thickness of the nitride layer. It should be noted that the stress in the nitride film is strongly dependent on the deposition conditions, which are different in the two experiments. However, they did observe a marked decrease in the net retardation as the width of the stripe was reduced, which concurs with the results of this study.

An increase in width of the nitride stripes, with the thickness remaining the same, leads to a decrease in the stress levels in the substrate in regions close to the interface. This was corroborated by FLOOPS simulations (Fig. 6). Therefore, with a tensile intrinsic stress in the nitride film, it is expected that the compressive pressure immediately below the nitride stripe would increase as the stripes are brought closer together (i.e., made smaller). This would decrease the local equilibrium concentration of interstitials in the region immediately below the nitride layer. Since phosphorus is known to diffuse mainly through an interstitial phenomenon, it is expected that the net retardation (ΔX_j) would increase as the stripes are made smaller and brought closer together. The results of this study, however, suggest some competing phenomenon is at work. A first order analysis of this phenomenon is presented in the subsequent paragraph.

The stripe width dependent stress analysis presented in the preceding paragraph is true for regions that are very close to the silicon/silicon-nitride or silicon/silicon oxide interface. For regions deeper in the substrate, the stress levels increase with increasing stripe width (Fig. 6). Since the junction staining technique is sensitive only to the junction depth in the sample, this competing mechanism is responsible for the increase in the net retardations with increasing stripe width.

For the $1 \mu\text{m}$ stripe width samples the net retardation (ΔX_j) falls to $\sim 400 \text{ \AA}$, and is at the resolution limit of the junction staining technique. For the widest stripes ($1000 \mu\text{m}$), the retardation increases almost threefold, to $\sim 1300 \text{ \AA}$.

The effect of a stress field on the local concentration of point defects is described by Eqs. (3) and (4). Thus, if a dopant-like phosphorus (known to diffuse mainly by an interstitial mechanism) is annealed in the presence of the nitride stripes, it should show a retardation in diffusion in regions of compression. While simulating the stress-assisted diffusion of phosphorus it is also important to incorporate the effect of the stress on the binding energy of the dopant-defect pair. The binding energy of a point defect pair is defined as the difference in the thermodynamic potential of the paired and unpaired point defect. Physically, the binding energy determines the number of point defect pairs that are present in the bulk. For the zero stress case, the binding energy is a constant dependent only on temperature. For the case when a nonzero stress field exists, the binding energy becomes dependent on the stress at any given location in the substrate. This makes the pairing coefficient a spatially varying quantity; the total number of point defect pairs in equilibrium are written⁸ as

$$C_{AX(P)}^* \cong C_{AX(P=0)}^* \exp\left(\frac{-P\Delta V_{AX}}{kT}\right), \quad (8)$$

where P is the hydrostatic pressure, and ΔV_{AX} are the effective volumes for elastic inclusion of dopant point defect pairs. Mathematically, it is positive for the interstitials and negative for the vacancies. Thus, the equilibrium concentration of phosphorus-interstitial pairs decreases, and phosphorus-vacancy pairs increases in a compressive medium. The model predicts a retardation in the diffusion of phosphorus in a compressive medium. The change in the point defect and dopant-point defect pair concentrations need to be simultaneously accounted for while simulating the stress-assisted diffusion of phosphorus.

Equation (8) brings out the effect of a stress field on the dopant-point defect pairs in the substrate and is implemented in FLOOPS by making the pairing coefficient a function of the pressure:

$$K_{AX(P)}^C = K_{AX(P=0)}^C \exp\left(\frac{-P\Delta V_{AX} + P\Delta V_X}{kT}\right), \quad (9)$$

where ΔV_{AX} and ΔV_X are positive for interstitials and negative for vacancies. Equation (9) implicitly accounts for the physics in Eq. (8). These equations are strongly sensitive to the effective volumes of the point defect and dopant-point defect pairs.

Under the annealing conditions used in the experiment, simulations showed that the effect of Eqs. (3), (4), and (9) on the diffusion of phosphorus is comparable. The volumes are extracted assuming the silicon interstitial to be a hypothetical sphere with radius equal to half the radius of single silicon atom. This is an approximation of the exact value, which should be the radius of the cavity into which the ‘‘self-interstitial’’ is inserted. For the vacancy volume, the effective radius r_s is assumed to be exactly equal to the radius of the missing atom. The value used for ΔV_{P_I} is estimated from

the radius of a hypothetical sphere with radius equal to the sum of the radii of a phosphorus atom and a silicon self-interstitial. The corresponding volume for a dopant-vacancy pair is more complicated to estimate, and is assumed to be twice that of the dopant-interstitial pair.⁸ Since the phosphorus diffuses almost entirely via an interstitial mechanism, the results of the simulations showed a weak dependence on the dopant-vacancy inclusion volumes. The stress levels in the nitride film are modified to account for the thermal strain at 1000 °C. The results of the simulations are directly compared with the experimental data in Fig. 4. The error bars for the measured data in the figure have been extracted by staining multiple samples from the same experimental split. This yields the bounds for the measured data. The discrepancy between the simulated and measured data points for the 20 $\mu\text{m}/2$ h sample in Figs. 4(a) and 4(b) is of the order of 50–100 Å, and is probably due to experimental error.

B. Simulation of stress-assisted evolution of dislocation loops

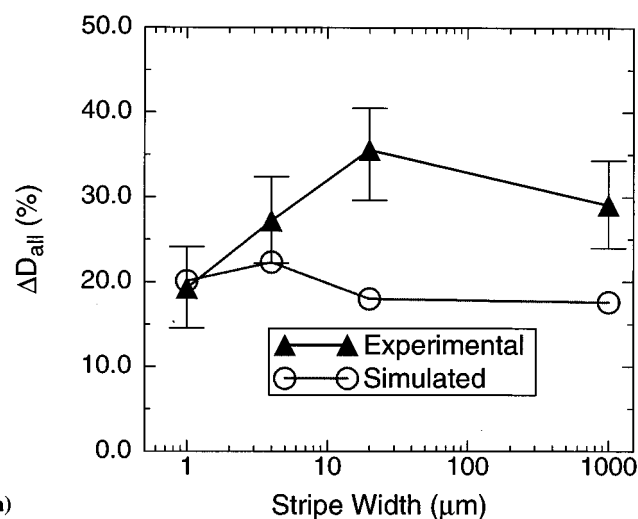
A model for the evolution of dislocation loops in an inert ambient, based on the Ostwald ripening phenomenon has been developed.⁷ The loss or gain of atoms during the anneal was found to be a strong function of loop size. Loops above a certain critical radius gained atoms and grew in size, while loops below the same critical radius lost atoms and eventually dissolved. This loss or gain of atoms for a given loop was also strongly dependent on the concentration of point defects in the bulk at its edge. In the presence of a pressure field the point defect concentrations are defined by Eqs. (3) and (4).

The continuity equation for the loss or gain of atoms for a loop with radius R ^{7,9} can now be rewritten by including the pressure dependence as

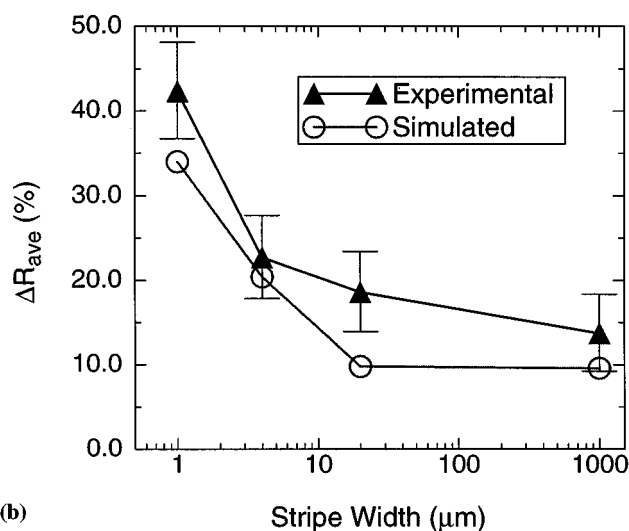
$$\left. \frac{\partial n}{\partial t} \right|_{\text{at Radius } R} = \alpha K_{IL} [C_I(P) - C_{Ib}] - \alpha K_{VL} [C_V(P) - C_{Vb}] \quad (10)$$

where α is an effective cross section of the loop layer in the unit of linear length, K_{IL} is the constant of reaction between the interstitials and the dislocation loops, K_{VL} is a similar constant for vacancies, $C_{I/V}(P)$ is the concentration of interstitials/vacancies in the presence of the pressure field, and $C_{Ib/Vb}$ is the number of interstitials/vacancies that a given dislocation loop can support at its edge.^{7,9}

In the presence of a pressure field the equilibrium concentration of point defects would change, altering their concentrations in the bulk, i.e., $C_{I/V}(P)$ is a function of pressure. Thus, Eq. (10) has an implicit pressure dependence. This implies that the rate of growth of the loops is now spatially dependent, dictated by the pressure field. To illustrate this point, assume that the pressure in a given region is compressive. The quantity on the left in Eq. (10) would decrease and, therefore, reduce the rate of growth of loops in that region. Similarly, the average rate of growth of loops in a tensile region would increase. This agrees qualitatively with the results of the experiment. Other loop ensemble properties, such as the maximum and minimum radius, and total loop density,



(a)



(b)

FIG. 7. The net variation (as a function of the stripe width) in (a) total density and (b) average radius of the dislocation loop ensemble, from a region where the nitride is directly on top of the silicon substrate to a region where an oxide layer pads of the underlying silicon from the deposited nitride.

change in accordance with the model described.⁷ Since the anneal was done at 900 °C, the parameters extracted⁷ are used again for the simulations.

The general procedure for characterizing dislocation loop ensembles in silicon has been discussed in detail.⁷ The peak radius (R_{peak}), average radius (R_{ave}), the density of loops with peak radius (D_{peak}), and the total density of loops (D_{all}), were used to characterize a dislocation loop ensemble. This procedure works well if the objective is to quantify the time evolution of a dislocation loop ensemble. However, in this experiment the goal is to investigate the stress-assisted evolution of dislocation loops. In particular, the focus is on the change in the properties of the loop ensemble from regions of compression (region B) to regions of tension (region A). To explain the effects observed in the experimental data the following three quantities are defined:

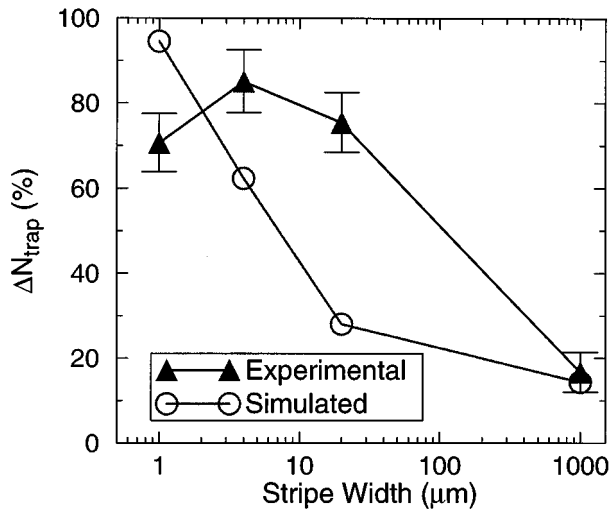


FIG. 8. The net variation (as a function of the stripe width) in the total number of trapped atoms in the dislocation loop ensemble, from a region where the nitride is directly on top of the silicon substrate to a region where an oxide layer pads of the underlying silicon from the deposited nitride.

- (i) $\Delta D_{\text{all}} \Rightarrow$ total density of loops in region A—total density of loops in region B.
- (ii) $\Delta R_{\text{ave}} \Rightarrow$ average radius of loops in region A—average radius of loops in region B.
- (iii) $\Delta N_{\text{trap}} \Rightarrow$ total number of trapped atoms in region A—total number of trapped atoms in region B.

Figures 7 and 8 illustrate this net variation in ΔD_{all} , ΔR_{ave} , and ΔN_{trap} as a function of the stripe width. As the stripes are brought closer together the net variation in the total density of the dislocation loops increases (for most cases), while the net variation in the average loop radius diminishes. Though the variation in ΔD_{all} is within error bars, the trend for the change in ΔR_{ave} and ΔN_{trap} is quite evident. As the stripe width is increased the stress level in regions immediately below ($<0.5 \mu\text{m}$) the silicon surface decreases (Fig. 6). This is reflected in the stripe width dependence of the loop ensemble properties (ΔR_{ave} and ΔN_{trap}).

These results are consistent with the hypothesis in the previous section: a compressive stress field in region B forces an increase in the equilibrium concentration of vacancies. Under these conditions an interstitial inside the loop is more likely to leave the ensemble and recombine with a vacancy outside the loop, or a vacancy might move into the loop and cause it to shrink. A reverse phenomenon is in effect in region A, which leads to bigger and denser loops in that region.

C. Validity of extracted volumes

The diffusivities of the dopant and point defects used for the simulations are their default values in FLOOPS. The effective volumes used for the simulations are consistent with Park *et al.*⁸ Since there is an exponential dependence of the bulk processing variables on these volumes, it is necessary to examine the validity of these parameters with the results of other researchers. This section examines the validity of the model and the methodology for extracting the effective dopant point-defect elastic inclusion volumes.

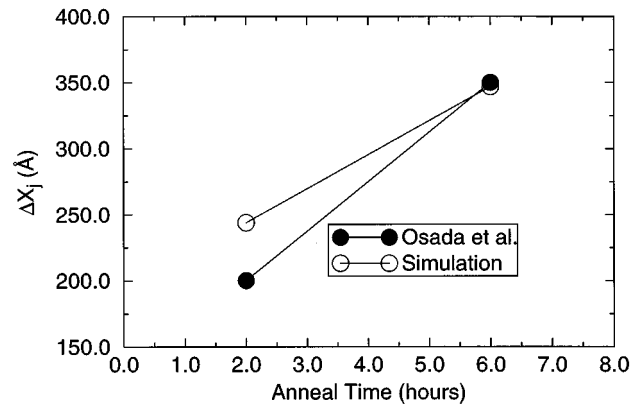


FIG. 9. Net retardation in diffusion (at 1041 °C), due to compressive stress in the substrate, for a $7.5 \times 10^{13}/\text{cm}^2$, 70 keV boron implant. The simulation is compared with data from Osada *et al.*

Osada *et al.*³ observed retarded diffusion of boron, when annealed under deposited nitride films. They suggested that a tensile stress of $\sim 1 \times 10^9$ dynes/cm² in the film was compressing the silicon below, thereby retarding the diffusion of the dopant. Although the effective volumes for the point defects are the same as the ones described earlier, the effective volumes for the dopant-point defect pairs are different for boron. To be consistent with the assumptions made while simulating the stress-assisted diffusion of phosphorus, the value used for ΔV_{BI} is estimated from the radius of a hypothetical sphere with radius equal to the sum of the radii of a boron atom and a silicon self-interstitial. The corresponding radius for a boron-vacancy pair is assumed, as before, to be twice that of the dopant-interstitial pair.

The results of the simulations are shown in Fig. 9. The implanted dopant is boron (70 keV, $7.5 \times 10^{13}/\text{cm}^2$) and the anneal is performed at 1014 °C for 2 and 6 h. The net retardation from the simulations matches well with the data from Osada *et al.*³ The experimental data indicate the absence of relaxation in the stress in silicon with time. This is probably because a major component of the stress is due to the thermal mismatch between the nitride and silicon substrate. This stress is present as long as the anneal temperature is maintained at 1014 °C.

V. CONCLUSION

The behavior of point defects under varying stripe widths of a nitride layer has been indirectly studied by observing the diffusion of phosphorus. The diffusion of phosphorus is retarded under regions where the nitride film is directly on top of the silicon substrate when compared to phosphorus diffusion in regions where an oxide pads off the silicon substrate from an overlying nitride film. As the stripes are made narrower and brought closer together this

net retardation decreases in magnitude. The anomalous diffusion is shown to be consistent with finite element stress and diffusion simulations.

The number of trapped atoms in a dislocation loop ensemble under a nitride film is found to be lower when compared to a region where the oxide layer pads off the underlying silicon substrate from the nitride film. As the stripes are made narrower and thus brought closer together the magnitude of this difference increases. The loops are always sparser and smaller under a nitride film. This anomalous behavior is consistent with the stress and loop evolution simulations in FLOODS.

ACKNOWLEDGMENTS

The authors would like to acknowledge Keith Rambo (lithography), Steve Schein (LPCVD nitridation),

James Chamblee (junction staining, Vishwanath Krishnamoorthy (TEM), and Semiconductor Research Corporation for funding this study.

- ¹ Shoichi Mizuo and Hisayuki Higuchi, *Jpn. J. Appl. Phys.* **21**, 281 (1982).
- ² S. T. Ahn, H. W. Kennel, J. D. Plummer, and W. A. Tiller, *J. Appl. Phys.* **64**, 4914 (1988).
- ³ K. Osada, Y. Zaitso, S. Matsumoto, M. Yoshida, E. Arai, and T. Abe, *J. Electrochem. Soc.* **142**, 202 (1995).
- ⁴ P. Kuo, J. L. Hoyt, and J. F. Gibbons, *Appl. Phys. Lett.* **66**, 580 (1995).
- ⁵ S. M. Hu, *J. Appl. Phys.* **70**, R53 (1991).
- ⁶ Mark E. Law, FLOODS/FLOODS Manual (1993–1995).
- ⁷ S. Chaudhry, J. Liu, M. E. Law, and K. S. Jones, *Solid State Electron.* **38**, 1313 (1995).
- ⁸ Heemyong Park, Kevin S. Jones, Jim A. Slinkman, and Mark E. Law, *J. Appl. Phys.* **78**, 3664 (1995).
- ⁹ Heemyong Park, K. S. Jones, and M. E. Law, *J. Electrochem. Soc.* **141**, 759 (1994).